Diffractive acoustic elements for laser ultrasonics

M. Clark, S. D. Sharples, and Michael G. Somekh
School of Electrical and Electronic Engineering, University of Nottingham, University Park, Nottingham NG7 2RD, United Kingdom

(Received 13 August 1999; revised 10 March 2000; accepted 15 March 2000)

Laser ultrasonics is an effective means of generating surface acoustic waves (SAWs). We have shown in previous publications how computer-generated holograms (CGHs) can be used to project optical distributions onto the sample surface. These can be used to control both the frequency content and the spatial distribution of the resulting ultrasound field. In this paper the concept is extended further to produce distributions which themselves act as diffractive acoustic elements (DAEs) for SAWs. It is demonstrated how frequency suppression, multiple foci, and frequency selective focusing of Rayleigh waves may be achieved with these elements. Agreement between the distributions predicted from the designs and those actually measured is excellent. © *2000 Acoustical Society of America.* [S0001-4966(00)05006-2]

PACS numbers: 43.38.Zp, 43.38.Rh, 43.35.Sx [SLE]

INTRODUCTION

Laser ultrasonics[1] enables samples to be tested in situations where access can be difficult and where coupling can be hazardous or degrade the measurement accuracy. The major disadvantage of laser ultrasonics over contacting technologies is that the sensitivity of optical detectors is poor compared to piezoelectric detection. This means that, in many cases, high laser powers have to be used to generate measurable ultrasonic amplitudes; this may lead to ablation of the surface. It is thus helpful if the total optical power used to generate the ultrasound is spread over the sample. Further improvements in the peak displacement can be achieved if the generated ultrasound is concentrated (focused) into a small region.

In order to increase the amplitude of the surface acoustic waves (SAWs) generated on the sample while minimizing the sample damage through ablation, two approaches have been used by previous authors. One method to increase the SAW amplitude involves passing the light from the generating laser through an axicon,[2] so that it focuses onto an annulus on the sample. This results in the generation of a converging (and diverging) surface acoustic wave, so that the amplitude of the surface acoustic wave at the center of the annulus is considerably increased. The second approach involves spreading the power of the generating beam using a moving grating formed by interfering two optical beams with slightly different frequencies.[3] Matching the wavelength of the grating to that of the surface wave at the difference frequency allows a strong ultrasonic signal to be generated with relatively low power density on the surface. Another related approach involves scanning a point line source at the phase velocity of the required surface wave.[4]

In this paper we discuss the design of a range of different computer-generated holograms (CGHs) which focus the SAW distributions as well as performing various filtering tasks on the ultrasonic distribution. The method is robust, allows extremely stable operation and, as we will show, is very flexible compared to other methods. We have reported previously on CGHs, which project an arc onto the surface of the sample, providing a diffraction-limited SAW (Rayleigh wave) focus.[5,6] These CGHs are analogous to using a refracting optical lens because they produce a continuous variation of the acoustic phase to effect the focusing. It is also possible to produce an analog of an optical diffractive CGH where control of the resulting beam is affected by discretely varying the phase of the ultrasonic source distribution. We describe continuous, discrete, and hybrid elements, which may be thought of as the Rayleigh wave analog of hybrid refractive/diffractive optical elements. We introduced the concept of diffractive acoustic elements (DAEs) and hybrid elements in Ref. 7; however, the present paper describes a wider range of elements performing many different tasks and we also describe special considerations that need to be borne in mind when designing these elements.

Section I describes the experimental setup and briefly discusses the method used to model the SAW distributions. In view of the distinction between continuous and discrete SAW elements, the rest of the paper is divided up as follows: Sec. II describes continuous distributions, used for focusing and frequency selection; Sec. III describes the application of discrete and hybrid distributions; Sec. IV discusses some of the design issues related to the discrete phase elements and considers the prospects for the elements discussed in this paper.

I. EXPERIMENTAL SETUP AND MODELING SAW DISTRIBUTIONS

The experimental setup used in this paper has been described elsewhere,[8] so a brief description will suffice. The system is shown schematically in Fig. 1. A mode-locked *Q*-switched laser was used to excite the ultrasonic beam. The laser produced a burst of approximately 30 short pulses each separated by 12 ns. Each burst was repeated every millisecond. The light from the source was then passed through different CGHs, which focused the beam onto the sample surface to form the profiles described throughout the paper. The resulting SAW distributions were detected with a specialized knife edge detector[6] which was mechanically scanned rela-

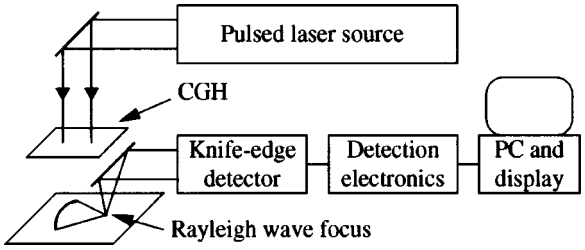

FIG. 1. Schematic diagram of laser ultrasound system. (CGH=computer-generated hologram.)

tive to the sample, while the illumination optics remained fixed. The peak envelope of the ultrasonic tone bursts were normally acquired using the envelope detection electronics described in Ref. 9.

The CGHs were designed using a direct search algorithm described elsewhere;[10] these produced the desired optical distributions on the sample surface. All elements were binary phase and etched in quartz. The CGHs profiled and shaped the laser beam so that no additional optical elements were required. The CGH thus replaces a focusing cylindrical lens in a conventional laser ultrasonic system.

In all the experiments the system operated in the thermoelastic regime and no surface treatment was performed on the samples. Inspection of the samples after the experiments revealed no detectable damage.

In order to predict the surface wave distributions expected from the samples, the predicted light distribution was calculated from the CGH design. This light distribution was then used to calculate the ultrasonic distribution close to the generation point. Since we are confident of always operating in the thermoelastic regime, the model of Krylov and Pavlov[11] was used, which predicts that the surface displacement due to Rayleigh wave motion, a_r, is given by the following relationship:

$$a_r \propto \frac{1}{\omega_r} F_s(k_r) F_t(\omega_r), \tag{1}$$

where $F_s(k_r)$ is the Fourier transform of the spatial distribution of the source intensity at the SAW wave number k_r and $F_t(\omega_r)$ is the corresponding temporal frequency component of the source at SAW frequency ω_r. This SAW distribution is then propagated along the sample using angular spectrum propagation as described by Goodman.[12] Here the scalar field of the SAWs at a line is decomposed into plane waves (the angular spectrum) by taking the Fourier transform of the complex amplitude of the SAW at the line. These plane waves are then propagated to the reconstruction line using an appropriate propagation factor, $\exp jk_r \cos\theta z$, where z is the propagation distance between the source and reconstruction line and θ is the angle between the plane wave and the axis of propagation (see Goodman[12]). The simulated SAW amplitude is then reconstructed from the resultant plane waves (by taking the inverse Fourier transform).

II. CONTINUOUS DISTRIBUTIONS FOR FOCUSING AND FREQUENCY CONTROL

A. SAW focusing

Focusing the Rayleigh wave distribution increases the displacement on the sample, thus improving the detectability of the surface wave distribution. In previous publications we have shown that this allows one to detect the ultrasonic distribution without averaging.[6,9] We have also shown how the increase in surface wave amplitude allows fast analog electronics to be used rather than a digital storage oscilloscope; this greatly improves the rate of image acquisition obtained in a noncontacting surface wave acoustic microscope.[9] The light distributions on the sample were obtained using a CGH, which produced a single arc. This provided focusing of the laser-generated surface waves, but offered little control of the frequency content of the resulting surface wave distribution. In this section the use of several concentric arcs is described; this increases the maximum power that the sample can withstand without ablation, thus providing an even greater enhancement of the SAW amplitude at the focus. The spacing of the arcs determined the frequency selection.

B. Frequency control: High pass filtering

Enhancing the harmonic signal and suppressing the fundamental can be important when trying to image at high frequencies where the signal at the fundamental is often much larger and may tend to swamp the desired harmonic. Figure 2 shows the SAW focus obtained at the focus of a four-arc distribution, which is shown schematically in Fig. 2(a). The separation between adjacent arcs is half a wavelength at 82 MHz and thus a whole wavelength at 164 MHz. This means that the excitation from each 82-MHz line cancels out, whereas the 164-MHz signals add in phase. The distributions shown in Fig. 2 clearly demonstrate this, since no 82-MHz signal can be detected above the noise in Fig. 2(b) and (d), whereas a diffraction-limited focus for the 164-MHz signal was observed in Fig. 2(c) and (d).

C. Frequency control: Low-pass filtering

Harmonic imaging involves excitation at a fundamental frequency and detection of the harmonic generated by nonlinearities in the sample. Harmonic imaging has been used in the fluid coupled scanning acoustic microscope but the large nonlinearity in the fluid means that more of the generation occurs in the couplant rather than the sample. In conventional fluid coupled acoustic microscopy, information about the couplant liquids and biological samples[13] may be obtained, but little information about the nonlinear acoustic properties of hard solid materials is accessible. Since laser ultrasonics does not use a couplant it is a promising technique for SAW harmonic generation in solid materials, particularly at cracks and discontinuities. The DAE described below is well-suited for such an application. To successfully perform harmonic imaging it is essential that any harmonic content in the input signal be suppressed so that it is not confused with the generated harmonic. To ensure efficient suppression of the harmonic a two-arc distribution was used

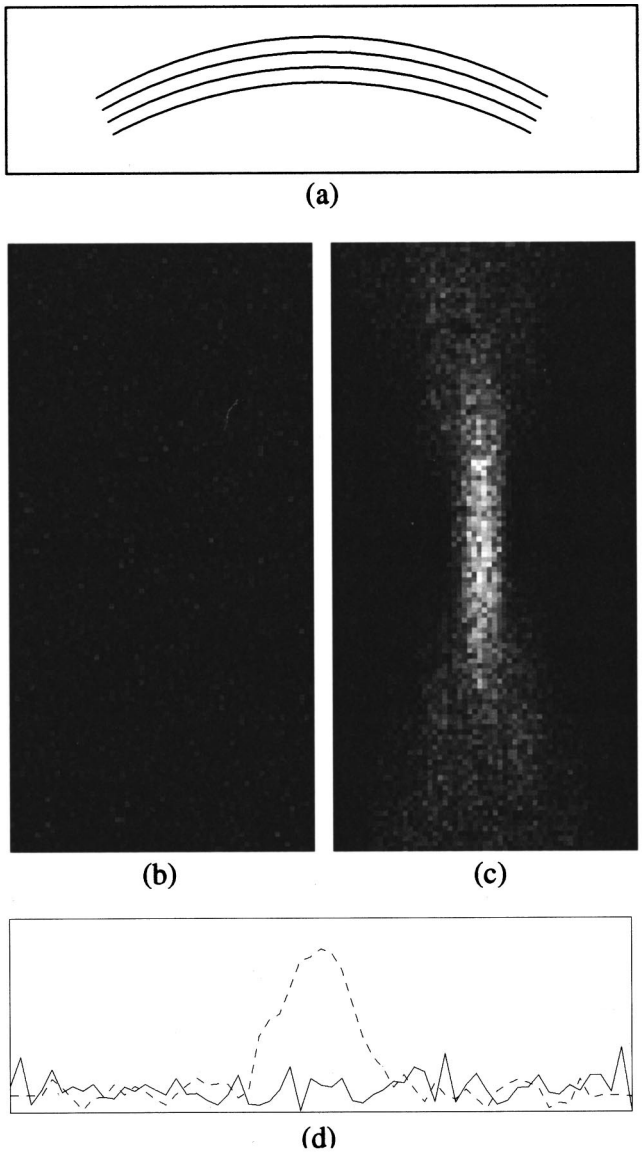

FIG. 2. Focus of a four-arc distribution, where each arc is separated by half a wavelength at 82 MHz. (a) Schematic of four-arc optical distribution; (b) no observable signal at 82 MHz; (c) strong diffraction-limited focus at 164 MHz; (d) Line plot through the focus, solid line 82 MHz, dashed 164 MHz. Image size 600 by 300 μm. Ultrasonic source 1 cm above center of image.

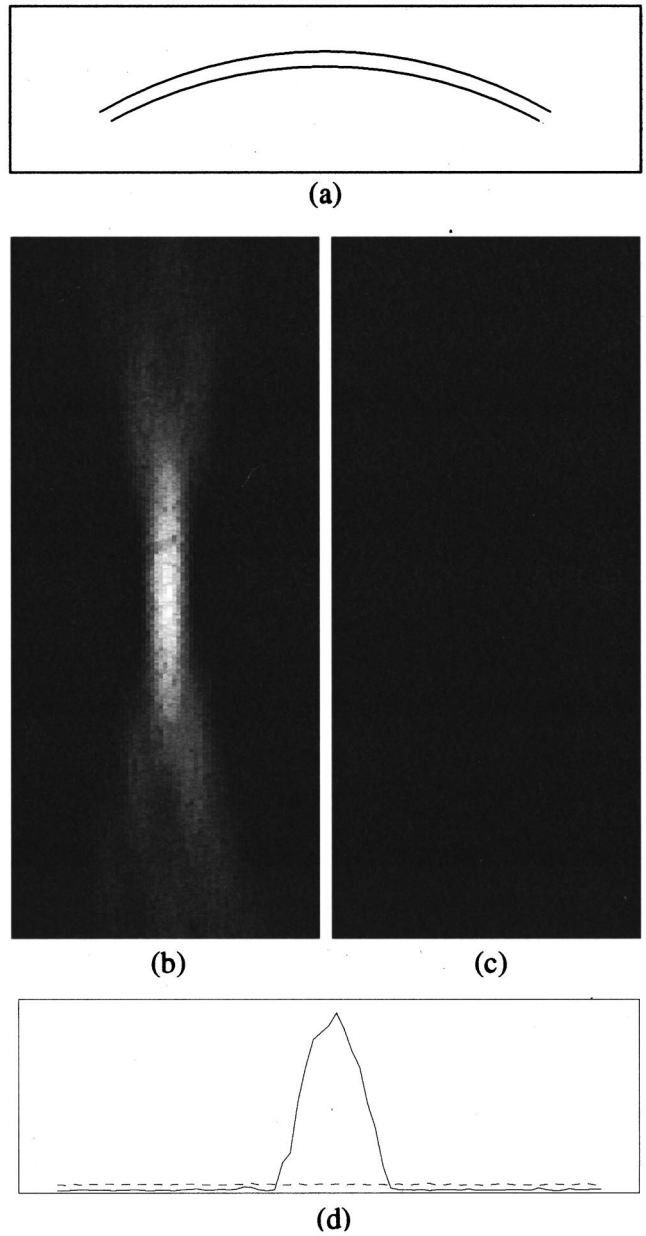

FIG. 3. Focus of two-arc hologram, where each arc is separated by three quarters of a wavelength at 82 MHz. (a) Schematic of two-arc optical distribution; (b) strong diffraction-limited focus at 82 MHz; (c) no observable signal at 164 MHz; (d) line plot through the focus, solid line 82 MH, dashed 164 MHz. Image size 600 by 300 μm. Ultrasonic source 1 cm above center of image.

[Fig. 3(a)]. In this case the arcs were separated by three half-wavelengths at 164 MHz, thus ensuring the cancellation of this signal. The separation at the fundamental frequency is therefore three quarter-wavelengths, so that the waves generated at 82 MHz from each line add in quadrature. This means that the amplitude of the resulting surface wave at the fundamental frequency has a large amplitude [see Fig. 3(b)] although it is reduced by a factor of $1/\sqrt{2}$ compared to the optimum case, in which all the contributing arcs add in phase rather than quadrature. On the other hand, the harmonic signal is suppressed, so that it is not visible above the noise [see Fig. 3(c) and (d)].

III. DISCRETE DIFFRACTIVE ACOUSTIC ELEMENTS

In Sec. II we showed how interference between SAWs could be used to suppress different frequency components; in this section we will show how CGHs may be used to produce discrete distributions, which themselves act as DAEs. DAEs, like optical diffractive elements, are very dispersive; this dispersion can be inconvenient or it can be useful to produce, for instance, frequency-dependent surface wave focusing.

A. Discrete acoustic element for focusing

In optics, one of the simplest diffractive elements is the binary phase plate, this introduces 180-deg phase shifts between adjacent zones, so that it acts as a ''discrete'' lens. For a binary (two-level) phase plate a parallel beam incident on the element will produce both a converging and a diverging beam from the $+1$ and -1 diffracted orders. Projecting an

array of short lines offset from each other by half the Rayleigh wave wavelength forms a DAE which acts as a surface wave analog of a zone plate [see Fig. 4(a)]. Ideally, this should produce a focus of SAWs. Figure 4(b) shows the predicted diffraction pattern from the ultrasonic phase plate of Fig. 4(a). The experimental focal plane distribution is shown in Fig. 4(c) and we note that the agreement is not particularly good. The reason for this is that there is a large path difference between extreme ray paths for this element. This path difference is approximately 1.4 mm, which corresponds to a relative time delay of 450 ns or 37 cycles of 82-MHz signal (the number of zones between the center and the edge of the phase plate). The large time delay means that all the surface waves do not interfere at the focus, due to the short duration of the *Q*-switched envelope (approximately 360 ns). This can be seen from the waveforms shown in Fig. 4(d). The top trace shows the compact waveform from a focusing arc; the middle trace shows the envelope at the focus obtained from the surface wave zone plate, where one may note the spreading; the bottom trace was obtained at the position of the expected first minimum of the focal distribution. This shows considerable spreading of the waveform as well as a phase dislocation, indicating that for a single frequency wave there would be phase cancellation. To perform effective interference it is necessary for the length of the individual pulse trains to be considerably longer than the maximum time delay between different paths. This can be achieved by passing the electronic signal through a very narrow bandpass filter. This was performed digitally by detecting the output ultrasonic waveform from the optical detector in the digital storage oscilloscope. Recall, that for the remaining measurements in this paper only the envelope of the output signal was detected. The waveforms detected at each scan point were then Fourier transformed and the component at 82 MHz was recovered. This was then used to form the corrected focal distribution, which is shown in Fig. 4(f), next to an expanded version of the theoretical distribution, Fig. 4(e). We can now see that the focal distribution from the phase plate agrees quite well with the expected distribution for a single frequency pulse.

B. Hybrid elements for frequency-dependent focusing

The simple phase plate is clearly unsatisfactory if we wish to use an envelope detector. The solution to this problem is to use a hybrid continuous/discrete DAE. In this case a weak phase plate was imposed on an arc as shown in Fig. 5(a). The arc forms the more powerful focusing element and the phase plate imposes a relatively weak perturbation; since the diffractive element imposed on the arc has only six zones between the center and the edge, effective interference can take place from our 30-cycle source. As mentioned earlier, the zone plate gives a $+1$ and a -1 diffracted order so that two foci are formed—one inside the geometrical focus of the arc and one outside. If the focal length of the arc is 10 mm and the focal length of the zone plate is 76 mm, we expect the two foci to be located at 8.8 and 11.5 mm, respectively. Figure 5(b) and (c) show excellent agreement between the simulated and measured focal distributions.

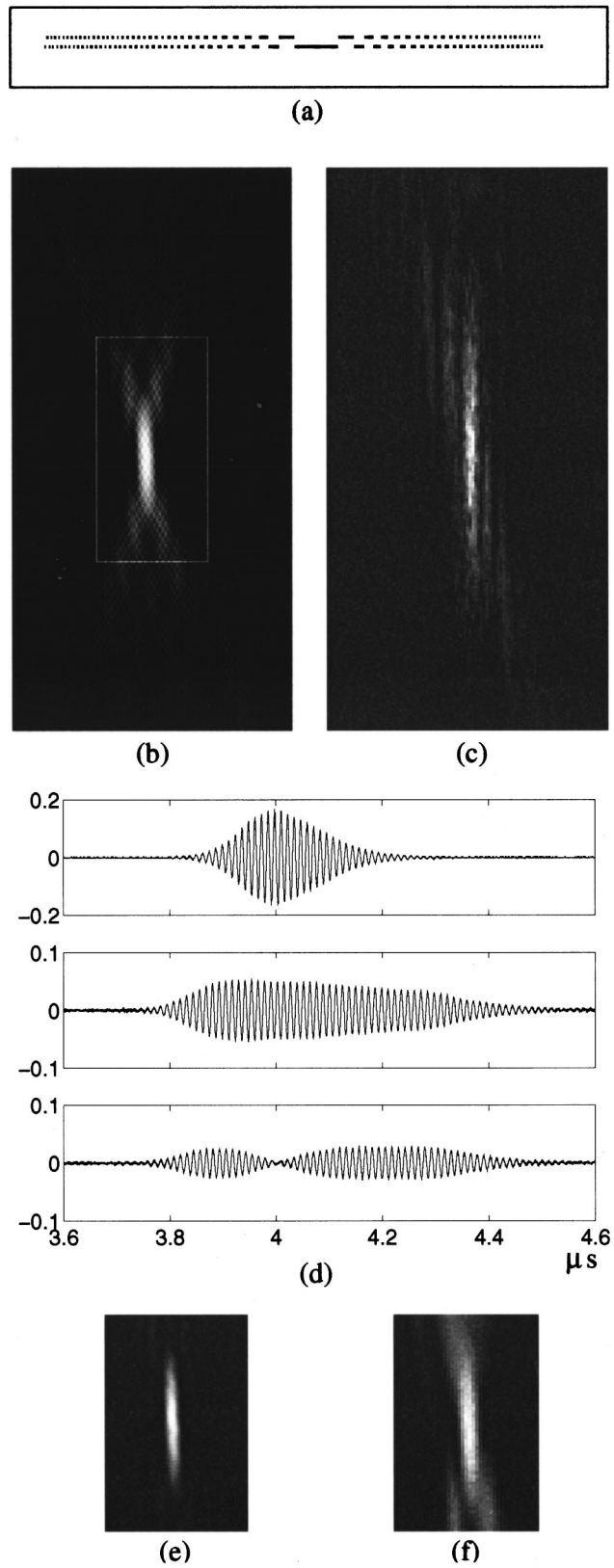

FIG. 4. Results obtained with acoustic zone plate. (a) Schematic of optical distribution; (b) predicted point spread function at focus. Image dimensions 2 by 1 mm; (c) measured point spread function, image dimensions as (b); (d) waveforms showing amplitude versus propagation time from generation source (microseconds). Top trace waveform at focus from an arc with same focal length, middle trace waveform at focus, bottom trace waveform at position of first zero (notice phase dislocation in waveform); (e) zoom of predicted point spread function (b), image size 600 by 400 μm; (f) measured point spread function after filtering. Image dimensions 600 by 400 μm.

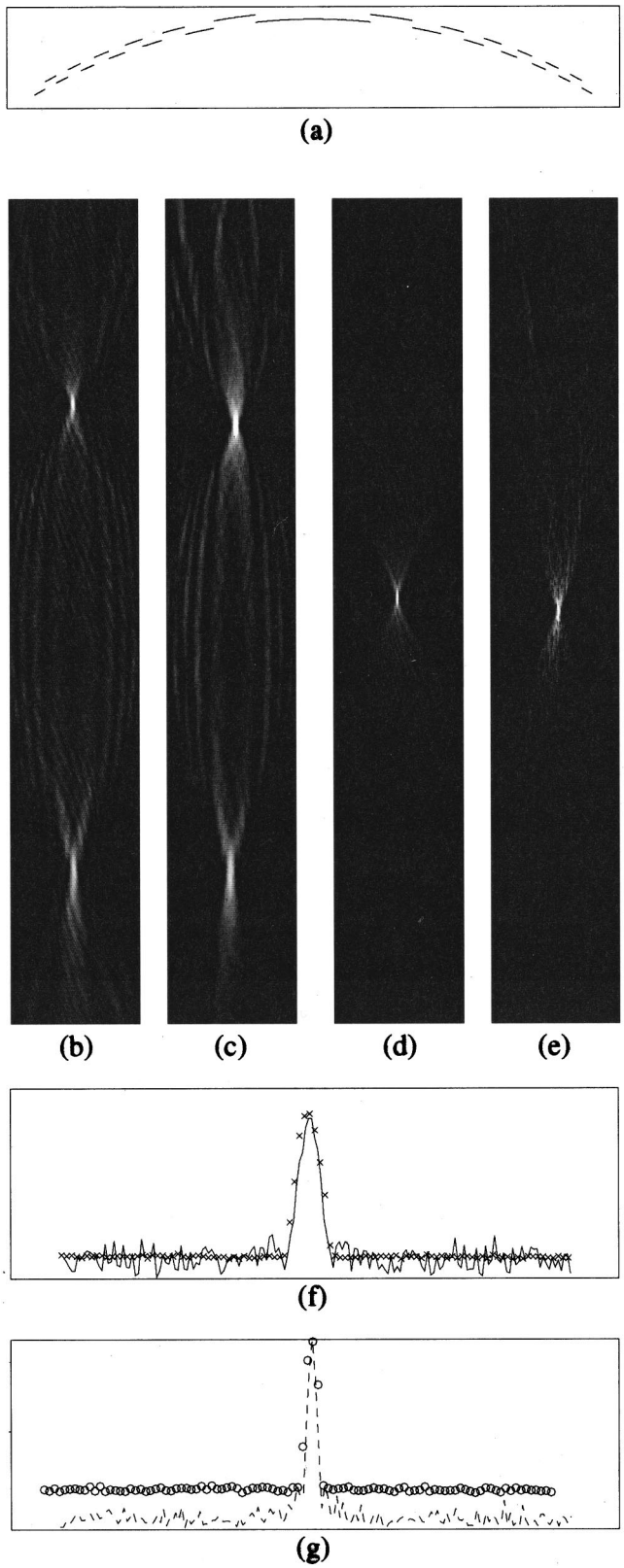

FIG. 5. Hybrid diffractive element with superimposed continuous wave front, with two focal lengths. (a) Schematic of optical distribution; (b) predicted focal distribution at 82 MHz; (c) measured distribution at 82 MHz; (d) predicted focal distribution at 164 MHz; (e) measured distribution at 164 MHz; (f) line plot through the first 82 MHz focus, solid line 82-MHz simulation, crosses measured SAW amplitude at 82 MHz. (g) line plot through the 164-MHz focus, dashed line 164-MHz simulation, circles measured SAW amplitude at 164 MHz. Image size 6.4 mm by 0.8 mm.

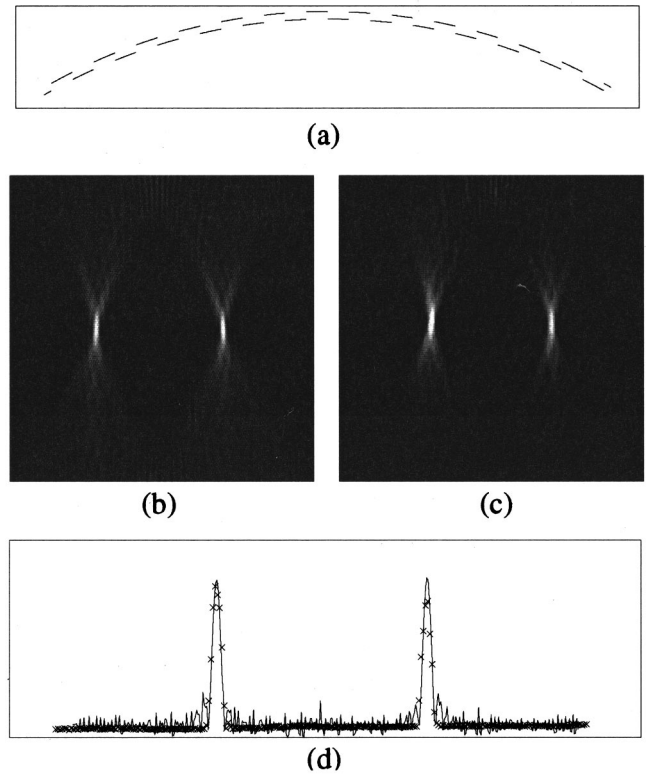

FIG. 6. Hybrid diffractive element with superimposed continuous wave front, with laterally offset foci. (a) Schematic of optical distribution; (b) predicted distribution from DAE showing laterally displaced foci at 82 MHz; (c) measured distribution from DAE showing laterally displaced foci at 82 MHz; (d) line plot through foci, solid line 82-MHz simulation, crosses measured SAW amplitude at 82 MHz. Image size 2.4 by 2.4 mm.

The half-wavelength phase delay at 82 MHz imposed by the displaced elements gives a whole wavelength relative delay at 164 MHz, so that the phase plate is ''invisible'' to the fundamental frequency. The focus for 164 MHz thus occurs at the geometrical focus of the arc. This is verified in Fig. 5(d) (predicted) and (e) (measured). The quantitative agreement between measured and predicted distributions may be determined from Fig. 5(f) and (g), which show the measured and predicted plots at 82 and 164 MHz, respectively.

C. Hybrid elements for displaced focusing

In addition to controlling the focal position along the axial direction, a combined continuous discrete element can also act as a Rayleigh wave analog of a Nomarski objective in optics, which forms two adjacent foci. This is achieved using an arc on which a grating is imposed [Fig. 6(a)], the $+1$ diffracted order introduces a phase tilt on the beam, which displaces the focus upwards and, similarly, the -1 order displaces the focus downwards. The simulations and the measured distributions are shown in Fig. 6(b) and (c), respectively, and a lineplot comparing experiment and theory is shown in 6(d); once again the agreement between experiment and theory is striking.

In order to demonstrate the flexibility of our approach we once again used a continuous arc with a superimposed discrete phase plate, but rather than maintain the symmetry

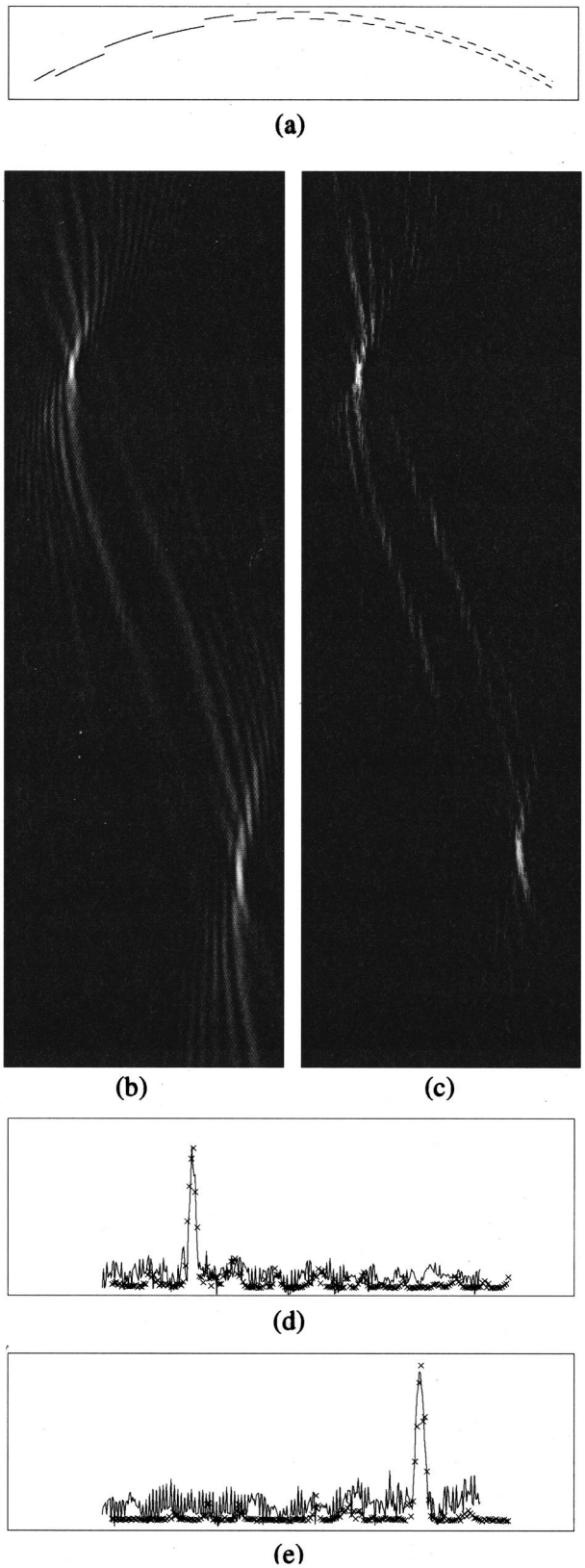

FIG. 7. Hybrid diffractive element with superimposed continuous wave front, with focuses offset both laterally and axially. (a) Schematic of optical distribution; (b) predicted distribution from DAE showing laterally and axially displaced foci; (c) measured distribution from DAE showing laterally and axially displaced foci; (d) and (e) line plots through first and second foci, respectively, solid lines 82-MHz simulation, crosses measured SAW amplitude at 82 MHz. Image size 6.4 by 2 mm.

of this phase plate about the axis the plate was displaced [Fig. 7(a)]. The +1 and −1 order focuses now differ not only in their axial position, but also in their height relative to the axis. Figure 7(b)–(e) show the excellent agreement between the simulated and measured distributions, even showing extremely close agreement in the fine detail of the wave distribution between the two foci.

IV. DISCUSSION

We have shown how from a specific optical design it is possible to generate an arbitrary optical distribution in the sample surface, which, in turn, acts as a Rayleigh wave diffractive element. The surface wave distribution is predicted entirely from the design of the optical element and gives excellent agreement. Combining curved sources with discrete phase plates gives control of the focal distributions and achieves multiple foci as well as frequency selective focusing.

We note that the DAEs described here differ from their optical counterparts in two important respects. First, the number of zones is by necessity rather small, to ensure good interference over a finite duration acoustic pulse; second, these DAEs are essentially one-dimensional—as opposed to two-dimensional—elements, since they are concerned with the focusing of SAWs. When phase plates are used in optics, the only criterion necessary to ensure suppression of the zero order is that there is 180-deg phase shift between adjacent zones. The large number of zones and the approximately equal areas in each zone—arising from the two-dimensional nature of the element—ensures that the areas corresponding to each phase shift are approximately equal. To ensure good zero-order suppression with DAEs, a little more care is required in the design, to ensure that the total line lengths (and hence generated SAW power) corresponding to each phase shift are approximately equal. In our designs the 0-order of diffraction is undetectable with a signal-to-noise ratio of 100:1 (at the peak of a focus).

In this paper we have concentrated our discussion on SAWs; however, concepts described here can also be applied to bulk waves. Projection of a distribution, which acts as a DAE for bulk waves, may be readily produced by projecting successive light and dark patches onto the sample. This element will act as an amplitude zone plate rather than a phase plate, but will produce a well-defined focus in the bulk of the sample. The methodology we have described has been applied to flat surfaces only, but the method should find application to curved surfaces, as the CGHs may be readily designed to produce a desired optical distribution over any arbitrary surface.

In future work we intend to use hybrid continuous/discrete elements to enhance the operation of a noncontacting SAW microscope and, in particular, examine the use of the frequency selectivity of these elements to facilitate harmonic imaging of defects.

ACKNOWLEDGMENTS

We are grateful to the Engineering and Physical Science Research Council and Rolls Royce plc for supporting this

work. The CGHs used in this study were designed in Nottingham and fabricated at Glasgow University.

[1] C. B. Scruby and L. E. Drain, *Laser Ultrasonics, Techniques and Applications* (Adam Hilger, Bristol, UK, 1990).

[2] X. Maldague, P. Cielo, and C. K. Jen, ''NDT applications of laser generated focused acoustic waves,'' Mater. Eval. **44**(9), 1120–1124 (1986).

[3] H. Nishino, Y. Tsukahara, Y. Nagata, T. Koda, and K. Yamanaka, ''Excitation of high-frequency surface acoustic-waves by phase-velocity scanning of a laser interference fringe,'' Appl. Phys. Lett. **62**(17), 2036–2038 (1993).

[4] K. Yamanaka, O. V. Kolosov, Y. Nagata, T. Koda, H. Nishino, and Y. Tsukahara, ''Analysis of excitation and coherent amplitude enhancement of surface acoustic-waves by the phase-velocity scanning method,'' J. Appl. Phys. **74**(11), 6511–6522 (1993).

[5] M. Liu, H. P. Ho, M. G. Somekh, and J. M. R. Weaver, ''Noncontacting optical-generation of focused surface acoustic-waves using a customized zoneplate,'' Electron. Lett. **31**(4), 264–265 (1995).

[6] F. Linnane, M. Clark, M. G. Somekh, and D. Zhang, ''Surface acoustic wave generation with customized optical beams,'' 1996 IEEE Ultrasonics Symposium, pp. 479–483.

[7] M. Clark, S. D. Sharples, and M. G. Somekh, ''Noncontact continuous wavefront/diffractive acoustic wave elements for Rayleigh wave control,'' Appl. Phys. Lett. **74**(24), 3604–3606 (1999).

[8] M. Clark, F. Linnane, S. D. Sharples, and M. G. Somekh, ''Frequency control in laser ultrasound with computer generated holography,'' Appl. Phys. Lett. **72**(16), 1963–1965 (1998).

[9] M. Clark, S. D. Sharples, M. G. Somekh, and A. S. Leitch, ''Noncontacting surface acoustic wave microscope,'' Electron. Lett. **35**(4), 346–347 (1999).

[10] M. Clark and R. Smith, ''A direct search method for the computer design of holograms,'' Opt. Commun. **124**, 150–164 (1996).

[11] V. V. Krylov and V. I. Pavlov, ''Thermooptical generation of surface acoustic waves in a solid,'' Sov. Phys. Acoust. **28**(6), 493–494 (1982).

[12] J. W. Goodman, *Introduction to Fourier Optics*, 2nd ed. (McGraw-Hill, New York, 1996).

[13] L. Germain and J. D. N. Cheeke, ''Generation and detection of high-order harmonics in liquids using a scanning acoustic microscope,'' J. Acoust. Soc. Am. **83**(3), 942–949 (1988).